

A non-monotonic constitutive model is not necessary to obtain shear banding phenomena in entangled polymer solutions

J. M. Adams¹ and P. D. Olmsted²

¹ *Cavendish Laboratory, University of Cambridge,
JJ Thomson Avenue, Cambridge, CB3 0HE, U.K.*

² *School of Physics & Astronomy, University of Leeds, Leeds, LS2 9JT, U.K.*
(Dated: February 10, 2022)

In 1975 Doi and Edwards predicted that entangled polymer melts and solutions can have a constitutive instability, signified by a decreasing stress for shear rates greater than the inverse of the reptation time. Experiments did not support this, and more sophisticated theories incorporated Marrucci's idea (1996) of removing constraints by advection; this produced a monotonically increasing stress and thus stable constitutive behavior. Recent experiments have suggested that entangled polymer solutions may possess a constitutive instability after all, and have led some workers to question the validity of existing constitutive models. In this Letter we use a simple modern constitutive model for entangled polymers, the Rolie-Poly model with an added solvent viscosity, and show that (1) instability and shear banding is captured within this simple class of models; (2) shear banding phenomena is observable for *weakly stable* fluids in flow geometries that impose a sufficiently inhomogeneous total shear stress; (3) transient phenomena can possess inhomogeneities that resemble shear banding, even for weakly stable fluids. Many of these results are model-independent.

PACS numbers: 83.80.Rs, 83.10.Kn, 83.60.Wc, 83.10.Gr

Much of the rheology of entangled polymers solutions and melts is captured by the molecular theory of Doi and Edwards (DE) [1], who argued that polymers relax by curvilinear diffusion (reptation) within a tube of the surrounding polymers. The DE model has a local maximum in the constitutive relation (the total shear stress as a function of shear rate for homogeneous flows). The resulting non-monotonic relation (*e.g.* the dashed curves in Fig. 2) leads to an instability that for many years was not observed in experiments [2], but nonetheless attracted attention [3, 4]. This stress maximum is predicted to be less pronounced or absent if the convected constraint release (CCR) of entanglements due to flow [5, 6, 7] is incorporated. A sudden release of a constraint can relax both the orientation and conformation of a stretched polymer, which increases the stress and, for sufficiently frequent events, eliminates the instability. The CCR mechanism also leads to neutron scattering predictions that agree with experiment [8]. Similar physics applies to solutions of breakable wormlike micelles, in which the instability is well documented experimentally and leads to *shear banding*, in which a fast-flowing oriented state coexists with a more disordered and viscous state along a stress plateau [9]. There, CCR is less pronounced because of breakage and fails to ameliorate a constitutive instability [7].

Recently, Wang, Hu and co-workers studied entangled solutions of a high molecular weight (HMW) polymer in its own oligomer [10, 11, 12, 13], or DNA solutions [14], finding a number of results that may be consistent with instability and shear banding after all. In controlled shear rate mode a weakly increasing stress plateau of three decades in shear rate was found, whereas in controlled shear stress mode the sheared solution experi-

enced a jump in the shear rate, together with spatially inhomogeneous birefringence [10]. Local velocimetry revealed spatially inhomogeneous velocity profiles in both the transient and the steady state [11] regimes, while large amplitude oscillatory shear flow (LAOS) experiments showed an inhomogeneous banding-like shear rate profile at finite frequencies [15]. Similar behavior was observed in a sliding plate shear cell in monodisperse solutions [12]. Relaxation after a step strain induced a highly inhomogeneous velocity field with *negative* local shear rates [13]. Hu *et al.* found similar inhomogeneous flow behavior and possible signatures of shear banding in polymer solutions, and wormlike micelle solutions at concentrations where severe shear thinning, but not banding, might be expected [16].

Wang *et al.* could not reconcile their results with existing theory, and proposed that the instability is a yield like effect due to an unbalanced “entropic retraction force” [17]. Here we show that much of the phenomenology of these experiments is consistent with the predictions of tube models with CCR, perhaps as anticipated in the original theory [3], without introducing new physics.

Model—We approximate the total stress \mathbf{T} as separating into fast Newtonian (or solvent) degrees of freedom and a slow viscoelastic component $\mathbf{\Sigma}$ (HMW polymer):

$$\mathbf{T} = -p\mathbf{I} + 2\eta\mathbf{D} + G\mathbf{\Sigma}, \quad (1)$$

where \mathbf{I} is the identity tensor, $\mathbf{D} = \frac{1}{2}[\nabla\mathbf{v} + (\nabla\mathbf{v})^T]$, p is the isotropic pressure determined by incompressibility ($\nabla \cdot \mathbf{v} = 0$), and η is the solvent viscosity, for which we use the dimensionless quantity $\epsilon = \eta/(G\tau_d)$. Here, τ_d is the reptation time. We are interested in the creeping flow (low Reynolds number) regime, in which $\nabla \cdot \mathbf{T} = 0$.

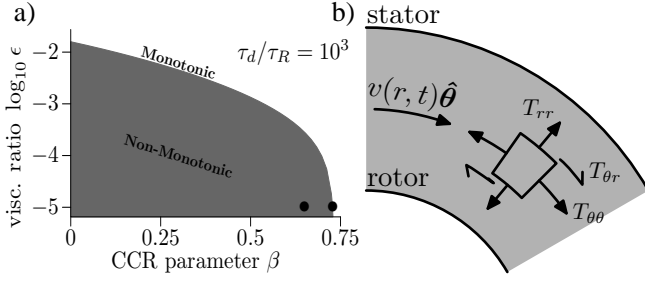


FIG. 1: a) Parameters (β, ϵ) where the constitutive curve of the Rolie-Poly model is non-monotonic (shaded). b) Section through Couette rheometer showing the flow field and total stress components, \mathbf{T} .

For the dynamics of Σ we use the Rolie-Poly (RP) model [6], a simplified tube model that incorporates CCR [7], where $\Sigma(\mathbf{r}, t)$ obeys

$$(\partial_t + \mathbf{v} \cdot \nabla) \Sigma + (\nabla \mathbf{v}) \cdot \Sigma + \Sigma \cdot (\nabla \mathbf{v})^T + \frac{1}{\tau_d} \Sigma = 2\mathbf{D} - \frac{2}{\tau_R} (1 - A) [\mathbf{I} + \Sigma(1 + \beta A)] + \mathcal{D} \nabla^2 \Sigma, \quad (2)$$

$A = (1 + \text{tr} \Sigma / 3)^{-1/2}$ and the Rouse time τ_R governs chain stretch. The stress “diffusion” term $\mathcal{D} \nabla^2 \Sigma$ describes the response to an inhomogeneous viscoelastic stress; while not in the original RP model, it can arise due to diffusion or finite persistence length [18, 19, 20]. We specify Neumann boundary conditions ($\nabla \Sigma = 0$) [20, 21]. From experimental values of the plateau modulus $G \sim 6 \times 10^2 \text{ Pa}$, reptation time $\tau_d \sim 20 \text{ s}$, and solvent viscosity $\eta \sim 1 \text{ Pa s}$ [10], we use $\epsilon = 10^{-5}$. Here we use $\tau_d / \tau_R \sim 10^3$, which is consistent with the length of the stress-shear rate plateau reported in [10]. The parameter β controls the efficiency of CCR, and is difficult to find a precise value of experimentally. Ref. [6] chose $\beta = 1$ to fit steady state data in polymer melts, and used multiple modes with $\beta = 0.5$ to fit experimental transient data. Here we tune between two qualitatively different types of constitutive curve; either a non-monotonic (0.65) or a monotonic (0.728) constitutive curve with a broad plateau (Figs. 1,2).

Eq. (2) was solved in one spatial dimension using the Crank-Nicolson algorithm [18], for unidirectional Couette flow $v(r, t)\hat{\theta}$ between cylinders of radii R_1 and R_2 parameterized by $q \equiv \ln R_2 / R_1$. In this geometry the total shear stress $T_{r\theta} \sim 1/r^2$, so that the stress difference across the flow cell is $\Delta \ln T_{r\theta} = 2q$. Cone and plate flow with cone angles of $\theta = (4^\circ, 1^\circ)$ has been reported [11, 16], so we use consistent values of stress difference corresponding to $q \simeq \Delta R / R = (2 \times 10^{-3}, 2 \times 10^{-4})$ [20]. Stresses are measured in units of G , shear rates in units of τ_d^{-1} , and velocities in units of $q R_1 / \tau \approx \Delta R / \tau_d$ for small q . To plot numerical data we use Γ , the dimensionless specific torque (per height per radian) on

the inner cylinder. The diffusion constant used was $\mathcal{D} \tau_d / (R_1 q)^2 = 4 \times 10^{-4}$.

Flow Curves—To calculate the steady state flow curves a step shear rate was applied from rest and evolved for $500 \tau_d$ with time step $10^{-5} \tau_d$, after which subsequent shear rate steps and time evolutions were applied to scan up and down in shear rate (Fig. 2). For non-monotonic constitutive curves ($\beta = 0.65$) shear banding always occurs, with hysteresis and a stress “plateau”. For the monotonic case ($\beta = 0.728$) shear banding could be inferred in the more highly curved geometry with the larger stress difference (larger q), since the flow curve no longer follows the constitutive curve; but *without* hysteresis. Crudely, a monotonic flow curve exhibits banding-like flows when most of the shear rate in the gap occurs over a small range of stresses, *i.e.* the slope of the plateau must be much smaller than the apparent slope specified by the flow geometry:

$$\left. \frac{d\Gamma}{d\dot{\gamma}} \right|_{\text{C.C.}} \ll \left. \frac{\Gamma(R_1) - \Gamma(R_2)}{\Delta \dot{\gamma}} \right|_g \sim e^q - 1, \quad (3)$$

where “C.C.” denotes the flat portion of the constitutive curve (dashed in Fig. 2) and “g” refers to the range of torques and shear rates specified by the flow geometry.

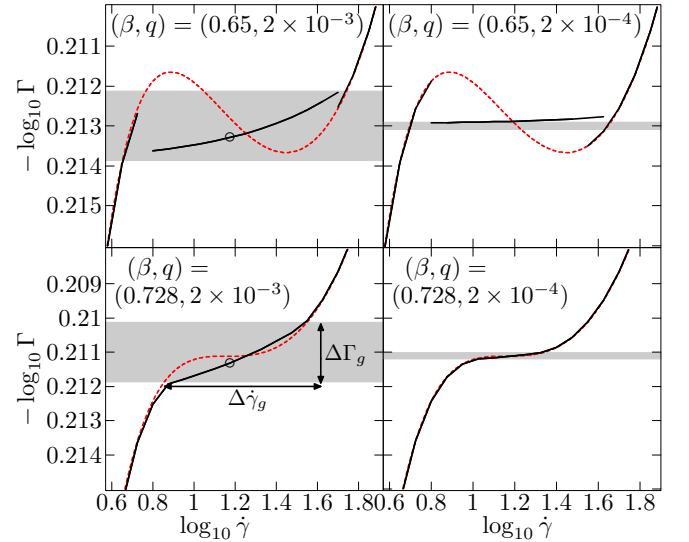


FIG. 2: Flow curves (solid black) and constitutive curves (dashed red) for a range of stress gradients q and CCR values β . The shaded area shows the size of the torque difference $\Delta \log_{10} \Gamma = \log_{10} e^{2q}$. Circles indicate applied shear rates at which the transient state responses are shown in Fig. 3.

The steady state velocity profiles are shown in Fig. 3 as solid (red) lines. The non-monotonic flow curves ($\beta = 0.65$) lead to a pronounced kink in the velocity profile, a signature of shear banding. The monotonic case does not shear band in the flatter geometry (small q), but for a more curved geometry (larger q) more shear

rates are accessible and the resulting smooth velocity profile could easily be interpreted as banding [11]; certainly the constitutive curve is not followed (Fig. 2). Similar smooth profiles were reported in [11, 16], in a flow geometry with $q \simeq 0.004 - 0.02$. A slightly increasing stress plateau over several decades in shear rates (as in [10]) would thus lead to apparently banding (inhomogeneous) flow in geometries with very low stress gradients; but a linear steady state profile is found if q is sufficiently small (Eq. 3).

Startup Transients—Transients were studied by evolving from rest using a time step of $10^{-5}\tau_d$ (Fig. 3). In all cases shown here strongly inhomogeneous flow develops after the stress overshoot, leading to a sharply banded transient state, with a *negative* velocity and shear rate in the less viscous band. In the monotonic case the velocity profile eventually smooths out. For a narrower stress plateau (e.g., $\beta = 0.3$, not shown) the overshoot has a less pronounced kink and typically a positive shear rate. We have found inhomogeneous transients with negative velocities with stress differences corresponding to a cone angle $\theta = 0.003^\circ$ in startup runs, but for $\theta = 0.001^\circ$ the amplitude of the inhomogeneous flow is reduced, and the velocity no longer negative, whilst for $\theta = 0^\circ$ the flow remains homogeneous. With perturbed initial conditions then the inhomogeneous transient behaviour returns. The transient for a monotonic model ($\beta = 0.728$) in which spatial gradients are artificially prohibited exhibits a slower decrease after the stress overshoot than in the spatially resolved model (Fig. 3); hence, inhomogeneities are important when using transient data to help differentiate candidate constitutive models [1, 22].

Large Amplitude Oscillatory Shear (LAOS)—A sinusoidal spatially-averaged shear rate was applied with frequency Ω and maximum shear rate $\dot{\gamma}_m$, and evolved from rest (zero stress) until any initial transients had decayed. We characterize the dynamics by the Weissenberg number $Wi = \dot{\gamma}_m\tau_d$ and the Deborah number $De = \Omega\tau_d$. For low De (frequency) we expect to recover some features of the steady state behavior, such as transient banding for Wi roughly within the non-monotonic part of the flow curve; while higher frequencies (high De) should produce sharper profiles similar to the transient behavior in Fig. 3, since the system cannot relax before flow reversal. At the highest frequencies we expect the reversing dynamics to be too fast to allow an inhomogeneous state.

Fig. 4A shows this behavior on a “Pipkin diagram” of Wi vs. De , for a monotonic flow curve ($\beta = 0.728$) in a slightly curved geometry. The inhomogeneous profiles in the banding regime (Fig. 4D) can be represented parametrically in terms of shear rate and torque, $(\dot{\gamma}(y), \Gamma(y))$ (Fig. 4B). At the high stress regions of the cycle a portion of the sample enters the high shear rate band as reported experimentally [15]. In these calculations the position y_* of the interface at a given strain $\dot{\gamma}_0/\Omega = 3$ varied with De as $y_* \sim (De)^\alpha$, where $\alpha \sim 0.4 - 0.6$, un-

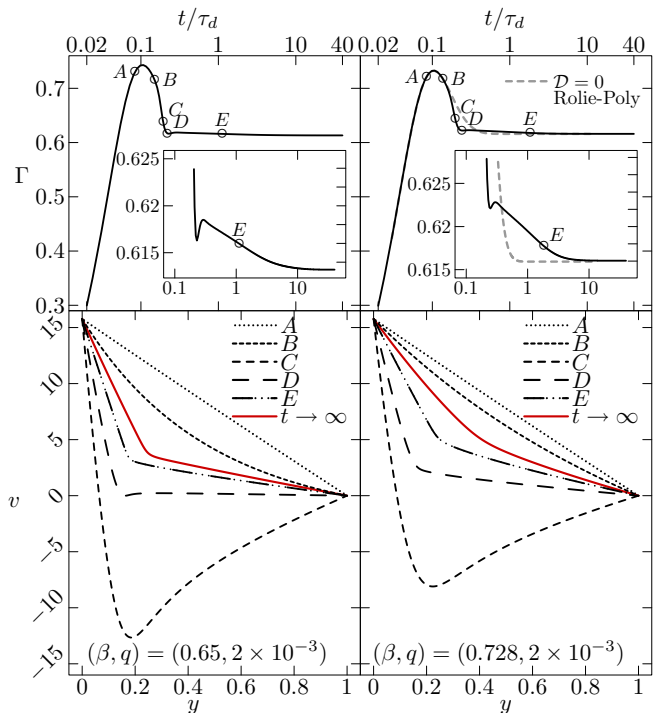


FIG. 3: Velocity as a function of position $y = q^{-1} \ln(r/R_1)$ for different (β, q) , at shear rate $\log_{10} \dot{\gamma} = 1.2$ (\circ in Fig. 2). The solid (red) lines indicate the steady state profile, and dashed lines are transient profiles at the times shown. The transient torque response in the spatially uniform model is shown for the monotonic case ($\beta = 0.728$) by a dashed line

like the fixed position reported in Ref. [15]. We suspect that these experiments did not attain steady state. The torque overshoot is typical of polymer solutions, and resembles that found in [16] (Fig. 4). At low frequencies the system has time to find a selected stress, which remains constant for part of the cycle while the shear band grows into the cell. At high frequencies the fluid cannot relax or shear band, which leads to a sinusoidal response and a nearly affine spatial profile.

Step Strain—Some experiments on the relaxation after a step strain found a strong inhomogeneous recoil that developed a negative velocity gradient [13]. We illustrate this with a monotonic constitutive curve ($\beta = 0.728$), Fig. 5. As in Fig. 5 of [13], an inhomogeneous velocity profile develops and the velocity becomes negative as the system recoils from the applied shear. Experimentally, the total displacement after recoil is of the order of a tenth of the gap size which is comparable with that observed here. Thus, inhomogeneities are important when using step strain data to help discriminate among candidate constitutive models, as when using the DE damping function [1, 22].

Summary—We have shown that behavior reminiscent of shear banding, as reported recently, can be reproduced

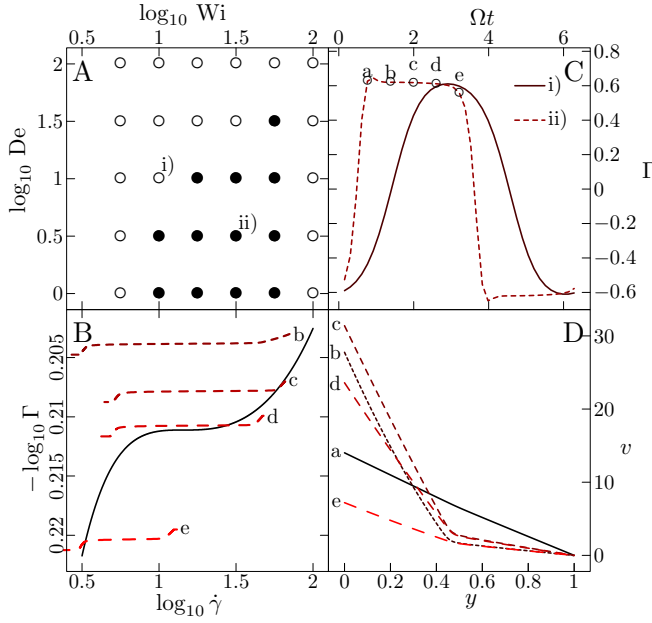


FIG. 4: (A) Pipkin diagram (Wi vs De) for $\beta = 0.728$ and $q = 2 \times 10^{-3}$, showing regions with homogeneous (\circ) and inhomogeneous profiles (\bullet). (B) Parametric shear rate-torque profiles ($\dot{\gamma}(y), \Gamma(y)$) (dashed: c,d) overlaying the constitutive curve (solid). (C) Torque evolution for different De noted on (A). (D) Velocity profiles for ii; profiles (a-e) are at different times in the cycle for $De \approx 3$ (ii) (\circ in C).

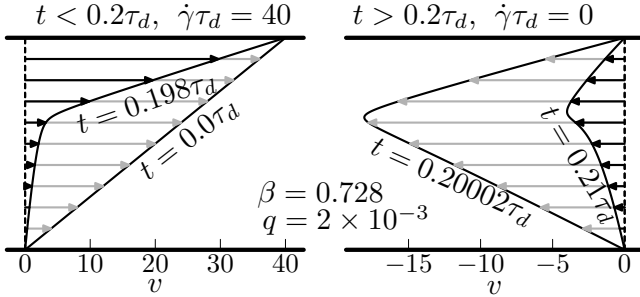


FIG. 5: Relaxation of a step strain of $\gamma = 8$, applied using $\dot{\gamma}\tau_d = 40$ for $t = 0.2\tau_d$. (Left) Velocity before the shear rate stops and (right) snap shots of recoil velocities.

using the Rolie-Poly model supplemented by a term to accommodate spatial gradients. The RP model contains an unknown parameter β , which controls the efficacy of convected constraint release. Even for β large enough to yield a stable (monotonic) constitutive curve, shear banding signatures can appear if the “stress plateau” is flat enough: (1) a geometry with a high stress gradient can induce a flow profile that could be mistaken for banding; (2) sharp banding-like profiles can appear in start-up transients even though the steady state is non-banded; (3) LAOS can trap these sharp transient profiles; and (4) relaxation after a large step strain can be very inho-

monogeneous, sometimes with a negative shear rate recoil. Several recent experiments, particularly on polydisperse polymer solutions, may fall into this category [16]. A wide plateau is believed to accompany very highly entangled systems [7], and the larger number of relaxation times are likely to render polydisperse systems intrinsically more stable than monodisperse systems [3], as was noted in recent experiments [16]. Our results are not specific to the RP model; Zhou *et al.* recently studied a different two-fluid model of shear banding (with a non-monotonic constitutive relation), and found qualitative results similar to some of ours [23].

We thank S.-Q. Wang, R. Graham, T. McLeish, O. Radulescu, and S. Fielding for lively discussions. This work was supported by the Royal Commission of 1851.

-
- [1] M. Doi and S. F. Edwards, *The Theory of Polymer Dynamics* (Clarendon, Oxford, 1989).
 - [2] R. A. Stratton, *J. Coll. Int. Sci.* **22**, 517 (1966); E. V. Menezes and W. W. Graessley, *J. Polym. Sci. Polym. Phys. Ed.* **20**, 1817 (1982); C. A. Hieber and H. H. Chiang, *Rheol. Acta* **28**, 321 (1989); C. Pattamaprom and R. Larson, *Macromolecules* **34**, 5229 (2001).
 - [3] M. Doi and S. Edwards, *J. Chem. Soc., Far. Trans. 2* **75**, 38 (1979).
 - [4] T. C. B. McLeish and R. C. Ball, *J. Poly. Sci. B-Poly. Phys.* **24**, 1735 (1986); T. C. B. McLeish, *J. Poly. Sci. B-Poly. Phys.* **25**, 2253 (1987).
 - [5] G. Marrucci, *J. Non-Newt. Fl. Mech.* **62**, 279 (1996); D. W. Mead, R. G. Larson, and M. Doi, *Macromolecules* **31**, 7895 (1998); G. Ianniruberto and G. Marrucci, *J. Non-Newton. Fluid Mech.* **95**, 363 (2000).
 - [6] A. E. Likhtman and R. S. Graham, *J. Non-Newt. Fl. Mech.* **114**, 1 (2003).
 - [7] S. T. Milner, T. C. B. McLeish, and A. E. Likhtman, *J. Rheol.* **45**, 539 (2001).
 - [8] J. Bent, L. R. Hutchings, R. W. Richards, T. Gough, R. Spares, P. D. Coates, I. Grillo, O. G. Harlen, D. J. Read, R. S. Graham, et al., *Science* **301**, 1691 (2003).
 - [9] N. A. Spenley, M. E. Cates, and T. C. B. McLeish, *Phys. Rev. Lett.* **71**, 939 (1993); M. E. Cates and S. M. Fielding, *Adv. Physics* **55**, 799 (2006).
 - [10] P. Tapadia and S. Q. Wang, *Phys. Rev. Lett.* **91**, 198301 (2003).
 - [11] P. Tapadia and S. Q. Wang, *Phys. Rev. Lett.* **96**, 016001 (2006).
 - [12] P. E. Boukany and S.-Q. Wang, *Journal of Rheology* **51**, 217 (2007).
 - [13] S.-Q. Wang, S. Ravindranath, P. Boukany, M. Olechnowicz, R. Quirk, A. Halasa, and J. Mays, *Phys. Rev. Lett.* **97**, 187801 (2006).
 - [14] P. E. Boukany, Y. T. Hu, and S. Q. Wang, *Macromolecules* **41** (2008).
 - [15] P. Tapadia, S. Ravindranath, and S. Q. Wang, *Phys. Rev. Lett.* **96**, 196001 (2006).
 - [16] Y. T. Hu, L. Wilen, A. Philips, and A. Lips, *Journal of Rheology* **51**, 275 (2007); Y. T. Hu, C. Palla, and A. Lips, *J. Rheol.* **52**, 379 (2008).

- [17] S.-Q. Wang, S. Ravindranath, Y. Wang, and P. Boukany, J. Chem. Phys. **127**, 064903 (2007); Y. Wang, P. Boukany, S.-Q. Wang, and X. Wang, Phys. Rev. Lett. **99**, 237801 (2007).
- [18] P. D. Olmsted, O. Radulescu, and C.-Y. D. Lu, J. Rheology **44**, 257 (2000).
- [19] A. W. El-Kareh and L. G. Leal, J. Non-Newt. Fl. Mech. **33**, 257 (1989).
- [20] J. M. Adams, S. M. Fielding, and P. D. Olmsted, J. Non-Newt. Fl. Mech. **151**, 101 (2008).
- [21] A. V. Bhave, R. C. Armstrong, and R. A. Brown, J. Chem. Phys. **15**, 2988 (1991).
- [22] S. Ravindranath and S. Q. Wang, Macromolecules **40**, 8031 (2007).
- [23] L. Zhou, P. A. Vasquez, L. P. Cook, and G. A. McKinley, J. Rheol. **52**, 591 (2008).